2156

Multi-modal multi-scale imaging reveals that long-association cortico-cortical systems are composed of short-range relay fibers

Chiara Maffei[1], Evan Dann[1], Robert Jones[1], Marina R. Celestine[2], Hui Wang[1], Suzanne Haber[2], and Anastasia Yendiki[1]
[1]Athinoula A. Martinos Center for Biomedical Imaging, Massachusetts General Hospital and Harvard Medical School, Charlestown, MA, United States, [2]Department of Pharmacology & Physiology, University of Rochester School of Medicine and Dentistry, Rochester, New York; Department of Psychiatry, McLean Hospital, Harvard Medical School, Belmont, MA, United States

Synopsis

Keywords: Tractography, White Matter, Structural Connectivity, Fiber Pathways

Motivation: Obtaining accurate anatomical information of connectional neuroanatomy across scales is crucial to improve *in-vivo*diffusion MRI techniques and advance our understanding of the brain white matter circuitries.

Goal(s): To reveal the mesoscopic organization of the SLF-I, a major cortico-cortical fiber association system of the human brain.

Approach: We combine multi-scale, multi-species, multi-modality connectional data from humans and macaques to investigate the structural connectivity of medial fronto-parietal cortical regions.

Results: We provide preliminary novel evidence that the SLF-I is composed of a succession of shorter relay fibers, which, in lower-resolution dMRI tractography result erroneously in a long, direct association bundle.

Impact: The mesoscopic anatomical validation of major white matter pathways in the human brain will increase the accuracy of their reconstruction in vivo, and open new avenues for our understanding of the functional substrates of these different connections.

Introduction

The current gap in spatial resolution between diffusion MRI (mm) and axons (µm) results in errors of dMRI tractography in regions with challenging fiber configurations[1]. Ex-vivo imaging allows us to obtain accurate anatomical information at higher resolution that can inform in vivo dMRI tractography[2]. Here we combine data across multiple modalities, scales, and species to clarify the connectivity of the dorsal branch of the superior longitudinal fasciculus (SLF-I), a major fiber association system running within the white matter of the superior frontal gyrus (SFG). Anatomic tracing studies in monkeys described the SLF-I as connecting the postero-medial parietal regions (PGm, PE, PEc) to different regions of the superior frontal gyrus (SFG) (6D, 8B, 9)[3]. Due to the complexity of SFG, where multiple projection systems merge with superficial U-fibers and frontal projections of the cingulum bundle, the morphology of the human SLF-I remains controversial. Tractography and post-mortem dissections have yielded conflicting results, some supporting direct, long connections from the parietal to the more frontal regions, and others supporting shorter or no SLF-I fibers[4,5]. Here, we combine multi-scale, multi-species, multi-modality data to investigate the mesoscopic organization within the SLF-I fiber system.

Methods

The different datasets used in this work are presented in Figure 1 and acquisition details are specified below.
Human data:
1) In vivo 1.5 mm dMRI: 3T MGH Connectom 1.0 Scanner, 2D EPI, 552 dMRI volumes (40 b=0, 64 b = 1000, 64 b = 3000; 128 b = 5000; 256 b = 10000 s/mm^2)[6].
2) In vivo 760 µm dMRI: 3T MGH Connectom 1.0 Scanner, gSlider-SMS, 2808 dMRI volumes (144 b=0, 420 b=1000, 840 b=2500 s/mm^2, paired reversed PE volumes)[7].
3) Ex vivo 750 µm dMRI: 3T Siemens Trio scanner, 3D diffusion-weighted SSFP, 68 dMRI volumes (TR=30.21 ms, TE=25.12 ms, 8 b=0, 60 b=4,000 s/mm^2).
4) Ex vivo 250 µm dMRI: 4 small blocks (roughly 2x2x1cm) were cut from dataset 3 and scanned on a 9.4T Bruker Biospec System (3D EPI, TR=75 ms, TE=43 ms, GRAPPA = 2, 515 dMRI volumes, maximum b = 40,000 s/mm2, 48 h).
5) PS-OCT 3 µm in plane: polarization-sensitive optical coherence tomography (PS-OCT) data were acquired on a system developed in-house [8].
Macaque data:
1) Ex vivo 700 µm dMRI NHP data: Small-bore 4.7T Bruker BioSpin scanner, 3D EPI sequence, 48h. 514 dMRI volumes (maximum b = 40, 000 s/mm^2)[1].
2) Tracer data: one male rhesus macaque received an injection in the frontal pole (10M), as described previously[9]. **Pre-processing**: All dMRI data were denoised using MP-PCA in MRtrix3[10] and corrected for motion/eddy current distortions in FSL[10]. We created a common parcellation scheme for macaque and human data to maximize anatomical comparison (Table 1). For each dataset, fiber orientation distributions were estimated using constrained spherical deconvolution[11] and connectivity matrices were generated (angle threshold:45°, step-size: 0.5 x voxel size) in MRtrix3[12]. PS-OCT data were processed as previously described[13] and tractography was performed using an in-house algorithm developed in Julia.

Results

Results show that most of the long, direct connections between parietal and frontal regions course within the cingulum bundle (white rectangles in figure 2), in accordance with the literature[14]. White-matter fibers originating in the parietal regions and coursing withing the SFG white matter mainly terminate in areas 4, 6, and 8B, as previously reported[2]. The number of direct, long connections coursing within the SFG white matter increases in lower resolution data (white square, figure 1). We qualitatively compared these long-range tractography reconstructions obtained from in vivo lower resolution dMRI data with four higher-resolution datasets: 1) virtual dissections of fibers coursing between the same areas obtained from high-resolution ex vivo dMRI data (750 and 250 µm); virtual dissections of fibers obtained from PS-OCT orientation data; virtual dissections of fibers in the ex vivo dMRI macaque data; anatomic tracer data in macaque (Figure 3). We found that all the higher-resolution datasets provide complementary evidence to support that the medial SFG has mainly short-range connections that come in and out the cortex, rather than long-range direct connections.

Conclusion

By comparing data across multiple modalities, scales, and species, we provide preliminary novel evidence that the SLF-I is composed of a succession of shorter relay fibers, which, in lower-resolution dMRI tractography result erroneously in a long, direct association bundle. These preliminary results point to the need to move beyond the conceptualization of white matter bundles as monolithic structures connecting wide portions of cortex and investigate the connectivity of the human brain at a finer scale. The delineation and characterization of these pathways will advance our understanding of the functional substrates of the brain connectome.

Acknowledgements

The research conducted in this work was supported by the National Institute of Biomedical Imaging and Bioengineering (R01-EB021265) and the National Institute of Neurological Disorders and Stroke (R01-NS119911, UM1NS132358-01). Additional support was provided by the National Institute of Mental Health (R01-MH045573, P50-MH106435).

References

1. Maffei C, Girard G, Schilling KG, [...], Yendiki A. Insights from the IronTract challenge: Optimal methods for mapping brain pathways from multi-shell diffusion MRI. Neuroimage. 2022 Aug 15;257:119327.

2. Yendiki A, Aggarwal M, Axer M, Howard AFD, van Walsum AVC, Haber SN. Post mortem mapping of connectional anatomy for the validation of diffusion MRI. Neuroimage. 2022 Aug 1;256:119146.

3. Petrides M, Pandya DN. Projections to the frontal cortex from the posterior parietal region in the rhesus monkey. J Comp Neurol. 1984 Sep 1;228(1):105-16.

4. Kamali A, Flanders AE, Brody J, Hunter JV, Hasan KM. Tracing superior longitudinal fasciculus connectivity in the human brain using high resolution diffusion tensor tractography. Brain Struct Funct. 2014 Jan;219(1):269-81.

5. Wang X, Pathak S, Stefaneanu L, Yeh FC, Li S, Fernandez-Miranda JC. Subcomponents and connectivity of the superior longitudinal fasciculus in the human brain. Brain Struct Funct. 2016 May;221(4):2075-92.

6. Fan Q, Witzel T, Nummenmaa A, Van Dijk KRA, Van Horn JD, Drews MK, Somerville LH, Sheridan MA, Santillana RM, Snyder J, Hedden T, Shaw EE, Hollinshead MO, Renvall V, Zanzonico R, Keil B, Cauley S, Polimeni JR, Tisdall D, Buckner RL, Wedeen VJ, Wald LL, Toga AW, Rosen BR. MGH-USC Human Connectome Project datasets with ultra-high b-value diffusion MRI. Neuroimage. 2016 Jan 1;124(Pt B):1108-1114.

7. Wang, F. et al. Motion-robust sub-millimeter isotropic diffusion imaging through motion corrected generalized slice dithered enhanced resolution (MC-gSlider) acquisition. Magn. Reson. Med. 80, 1891–1906 (2018).

8. Wang H, Akkin T, Magnain C, Wang R, Dubb J, Kostis WJ, Yaseen MA, Cramer A, Sakad ž i ć S, Boas D, 2016. Polarization sensitive optical coherence microscopy for brain imaging. Opt. Lett 41 (10), 2213–2216.

9. Lehman JF, Greenberg BD, McIntyre CC, Rasmussen SA, Haber SN, 2011. Rules ventral prefrontal cortical axons use to reach their targets: implications for diffusion tensor imaging tractography and deep brain stimulation for psychiatric illness. J. Neurosci. 31, 10392–10402.

10. Andersson, J. L., Skare, S., & Ashburner, J. (2003). How to correct susceptibility distortions in spin-echo echo-planar images: application to diffusion tensor imaging. Neuroimage, 20(2), 870-888.

11. Daan Christiaens, Ben Jeurissen, Chun-Hung Yeh, Alan Connelly. MRtrix3: A fast, flexible and open software framework for medical image processing and visualisation, NeuroImage,2019, 202; 116137.

12. Tournier, J.-D, Calamante, F. and Connelly, A. Improved probabilistic streamlines tractography by 2nd order integration over fibre orientation distributions. Proceedings of the International Society for Magnetic Resonance in Medicine, 2010, 1670.

13. Jones R, Maffei C, Augustinack J, Fischl B, Wang H, Bilgic B, Yendiki A. High-fidelity approximation of grid- and shell-based sampling schemes from undersampled DSI using compressed sensing: Post mortem validation. Neuroimage. 2021 Dec 1;244:118621.

14. Heilbronner SR, Haber SN. Frontal cortical and subcortical projections provide a basis for segmenting the cingulum bundle: implications for neuroimaging and psychiatric disorders. J Neurosci. 2014 Jul 23;34(30):10041-54.

15. Calabrese E, Badea A, Coe CL, Lubach GR, Shi Y, Styner MA, Johnson A (2015) "A diffusion tensor MRI atlas of the postmortem rhesus macaque brain" Neuroimage 117:408–416[16] Tang W, Jbabdi S, Zhu Z, Cottaar M, Grisot G, Lehman JF, Yendiki A, Haber SN, 2019. A connectional hub in the rostral anterior cingulate cortex links areas of emotion and cognitive control.

Figures

Macaque	Human		Anatomical Definition
CIVM Atlas	FS Parcellation	Petrides	
F2, F7, 6M (SMA)		6	Premotor
9L		9L	dlPFC
9M		9M	dmPFC
8B		8B	FEF
10dorsal, 10medial, FP		10M	Anterior PFC, FP
4		4	Primary Motor Cortex
9/46d		9/46d	dlPFC
31	Posteriorcingulate		Posterior Cingulate Gyrus
1/2 Somatosensory	Postcentral		Post Central Gyrus
PGM/31	Precuneus		Precuneus
PE, PEc	Superiorparietal		Superior Parietal Lobule

Table 1. Correspondence of anatomical regions used to create a common parcellation scheme of the dorsomedial cortex in macaque and human data. For macaque data, regions were derived from the Calabrese et al. (2015) MRI and DTI macaque atlas[15]. For the human datasets, we combined the FreeSurfer parcellation with a publicly available parcellation scheme that translates anatomical definitions of cytoarchitectonic regions of the frontal cortex to the fsaverage cortical surface[16].

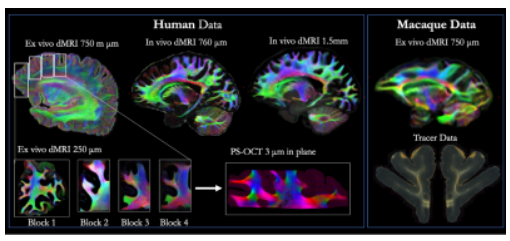

Figure 1. Dataset overview. Color encoded direction maps obtained from the estimated fODFs are shown for each of the MRI datasets for both human and macaque data. A representative optic axis map obtained from polarized-sensitive optical coherence tomography (PS-OCT) data and a photomicrograph from anatomic tracer data are also shown.

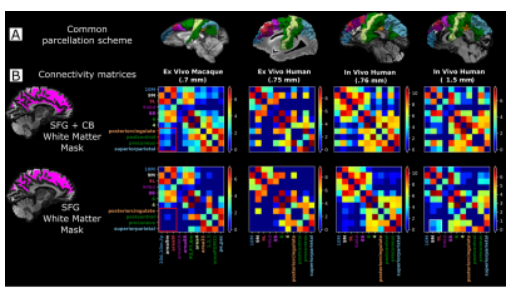

Figure 2. A) Common parcellation scheme of medial pre-frontal, cingulate, and parietal cortex across scales and species. B) Connectivity matrices between regions shown in A) computed using streamlines coursing through both SFG and cingulum bundle (CB) white matter (top row) and SFG white matter only (bottom row). Regions are displayed in an anterior-to-posterior order. Number of streamlines connecting regions is expressed as log(n).

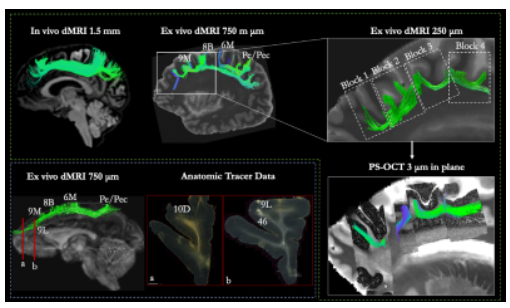

Figure 3. Long, direct connections obtained in lower resolution (1.5 mm) in-vivo tractography are compared to tract virtual dissections in higher resolution ex-vivo data (750 and 250 µm) and polarization-sensitive optical coherence tomography (PS-OCT), and to anatomic tracer data in one macaque sample. Tracer data show fibers leave the injection in the frontal pole and move superior **(a)** to reach 10D and then travel posteriorly to terminate in regions 9L and 46 **(b)**,without continuing more posteriorly. Red lines indicate the approximate position of the photomicrographs.